OPEN ACCESS

Energy Storage LETTER

The Innovation Energy

Dynamic photovoltaic power tracking exploration: Efficient synergy of thermal storage air-conditioning and micro-battery energy storage

Yuchen Liu,[1] Jingyu Cao,[1,2,5,*] Qiliang Wang,[3] Jian Li,[4] Gang Pei,[3] Jie Ji,[3] and Jinqing Peng[1,5,*]

[1]College of Civil Engineering, Hunan University, Changsha 410082, China

[2]Greater Bay Area Institute for Innovation, Hunan University, Guangdong 511300, China

[3]Department of Thermal Science and Energy Engineering, University of Science and Technology of China, Hefei 230026, China

[4]School of Mechanical Engineering, Beijing Institute of Technology, Beijing 100081, China

[5]Key Laboratory of Building Safety and Energy Efficiency of Ministry of Education, Hunan University, Changsha 410082, China

*Correspondence: jqpeng@hnu.edu.cn (J. P.); jycao@hnu.edu.cn (J. C.)

Received: June 6, 2026; Accepted: July 22, 2026; Published Online: July 23, 2026; https://doi.org/10.59717/j.xinn-energy.2026.100177

© 2026 The Author(s). This is an open access article under the CC BY license (https://creativecommons.org/licenses/by/4.0/).

Citation: Liu Y., Cao J., Wang Q., et al. (2026). Dynamic photovoltaic power tracking exploration: Efficient synergy of thermal storage air-conditioning and micro-battery energy storage. *The Innovation Energy* **3**:100177.

Dear Editor,

As electricity demand rose and renewable energy was integrated at large scale, grid stability faced increasing challenges.[1] Demand response (DR) showed value through load shifting to mitigate photovoltaic (PV) volatility.[2] Buildings accounted for about 30% of global energy consumption.[3] Energy storage and air-conditioning, dominating building energy systems, had been widely studied for its high flexibility.[4-5] However, most studies remained simulated-based for single energy storage in air-conditioning and lacked experimental verification of hybrid storage flexibility.[6-8]

In this letter, a cost-effective hybrid energy storage concept combining thermal energy storage (TES) and micro-battery energy storage (BES) was proposed to synergistically improve both the capacity and quality of system flexibility. The laboratory in Changsha covers about 66.56 m^2 with PV installation of 8 kW and a lithium-ion battery of 12 kWh and two water tanks of 3 m^3. The system primarily comprised PV-BES, central air-conditioning (CAC), water tank, and grid (Figure 1A). The water piping systems for CAC and TES were connected in parallel to enable slow, large-capacity scheduling, while PV-BES provided rapid, small-capacity compensation to offset thermal-side imprecision. The grid served as backup. A tiered response framework from seconds to hours was formed through coordinated control among the four components, aiming to experimentally verify the dual improvement of flexibility and renewable energy absorption quality under micro-BES storage.

On this basis, a CAC load scheduling system integrated water-based TES with BES was developed (workflow in Figure 1B). A load scheduling mechanism coupling three flexible resources was proposed. The focus was first on tracking PV output during the rising/falling phases by scheduling building thermal mass (BTM) or TES together with BES. Load scheduling was primarily achieved through temperature regulation (TR) and TES charging/discharging, while BES provided precise supplementary power based on PV output. The scheduling characteristics and flexibility quality of each source were evaluated to inform the analysis of full-day tracking experiments under different PV volatility. Finally, optimized DR strategy recommendations were summarized for various scheduling requirements.

To explore the scheduling characteristics of thermal-side DR strategies and PV consumption feasibility with micro-BES, PV tracking experiments were first conducted using single strategies (Figures 1C–F). Thermal-side flexible resources provided considerable flexibility, improving PV tracking versus baseline. The TR strategy, limited by BTM capacity, showed inadequate tracking capabilities. The maximum power under pre-cooling was 4.164 kW, and the minimum under global temperature adjustment (GTA) was 3.096 kW. TES offered greater flexibility, maintaining good alignment with both high and low PV power, though precise matching was not achieved by TES alone. The green dashed line represented the sum of CAC and battery power during DR. The inset (Figure 1D) showed that tracking errors were significantly reduced after BES intervention. After reaching rated power, CAC entered a prolonged stable phase. Flexibility mainly appeared as slow power changes. A gear shift occurred only when load scheduling became sufficiently large. The potential for more precise or rapid scheduling was then examined by analyzing coordinated scheduling of BTM and TES (Figures 1G–J). Greater regulation capacity was demonstrated in Cases 5 and 6 due to the combined effect of BTM and TES, allowing CAC to exceed the rated power limit. In Cases 7 and 8, the limited BTM flexibility served as a buffer against strong TES-based adjustments, making CAC power variations easier to control. For example, in Case 7, the initial load was reduced by GTA, stabilizing early tracking. Leveraging the buffering effect of TR, gradual power changes and smooth transitions were achieved in both Cases 7 and 8. Nevertheless, BES was still required for more precise and rapid PV tracking.

During experiments, rooms were kept in the comfort range of 21.9~25.6 °C (setpoint: 21~27 °C). However, it was worth considering that DR strategies could be influenced by indoor loads. Particularly, the scheduling of BTM, was significantly affected by indoor loads. Further details on cooling capacity, indoor/outdoor conditions, and tank status were in the supplementary document.

Figure 1K illustrated PV integration performance of thermal-side DR strategies. Differences in results are caused by morning-afternoon indoor load variations. In the morning, self-consumption rate (SCR) was improved by thermal-side DR strategies, and self-sufficiency rate (SSR) was reduced slightly. The afternoon showed the opposite. The Power matching index (PMI) of all strategies was improved to different degrees. Among them, the pre-cooling strategy performed well in morning PV consumption (SCR and SSR > 97%). However, it demonstrated disadvantages in load scheduling capacity and response speed, achieving only a 12.6% increase in SSR and an PMI of 1.22 compared to the baseline. TES-based DR strategies (Cases 3 and 4) further improved SCR in the morning and SSR in the afternoon (98.3% and 97.2%). Coordinated strategies (Cases 5-8) retained the PV tracking advantage of TES-based DR strategies (SCR and SSR > 94%). In terms of PMI, all thermal side DR strategies except the GTA strategy remained within 0.95 ~ 1.04. Notably, after the combination with BES, the system SCR and SSR under all strategies reached over 99.8%.

As a high-cost component, BES price was identified as a critical factor for system feasibility. Battery capacity and rated power were key cost drivers.[9] Cost estimates, based on maximum power and capacity requirements from Figure 1L, showed that Cases 4 and 5 achieved the lowest costs (¥307.53 and ¥666.41). Lower capacity consumption and better Energy efficiency (EE) were shown in Case 1, but higher maximum power increased costs. Morning PV consumption required larger load scheduling capacity and faster response, necessitating combined pre-cooling and TES charging. Afternoon PV tracking placed lower demands. In Case 8, comprehensive improvements were achieved through the interaction of pre-cooling and TES discharging, demonstrating feasibility under steady-state DR events.

In actual operation, PV curves often exhibited sharp decline, rapid rise, and jagged fluctuations. However, temperature control logic was restricted by room temperature feedback, producing delays that hindered rapid scheduling.[10] In contrast, direct wind-speed control allowed faster BTM scheduling. Combined with the buffering effects of TES and BES, this strategy showed greater potential for multi-scenario PV tracking throughout the day. To explain the response mechanism under different fluctuation conditions, two typical cases (low and high volatility) were selected for full-day PV tracking experiments, with power fluctuation range ratio of 9.9 and 15.5, respectively. The tracking performance and strategy implementation were summarized in Figures 1M & N.

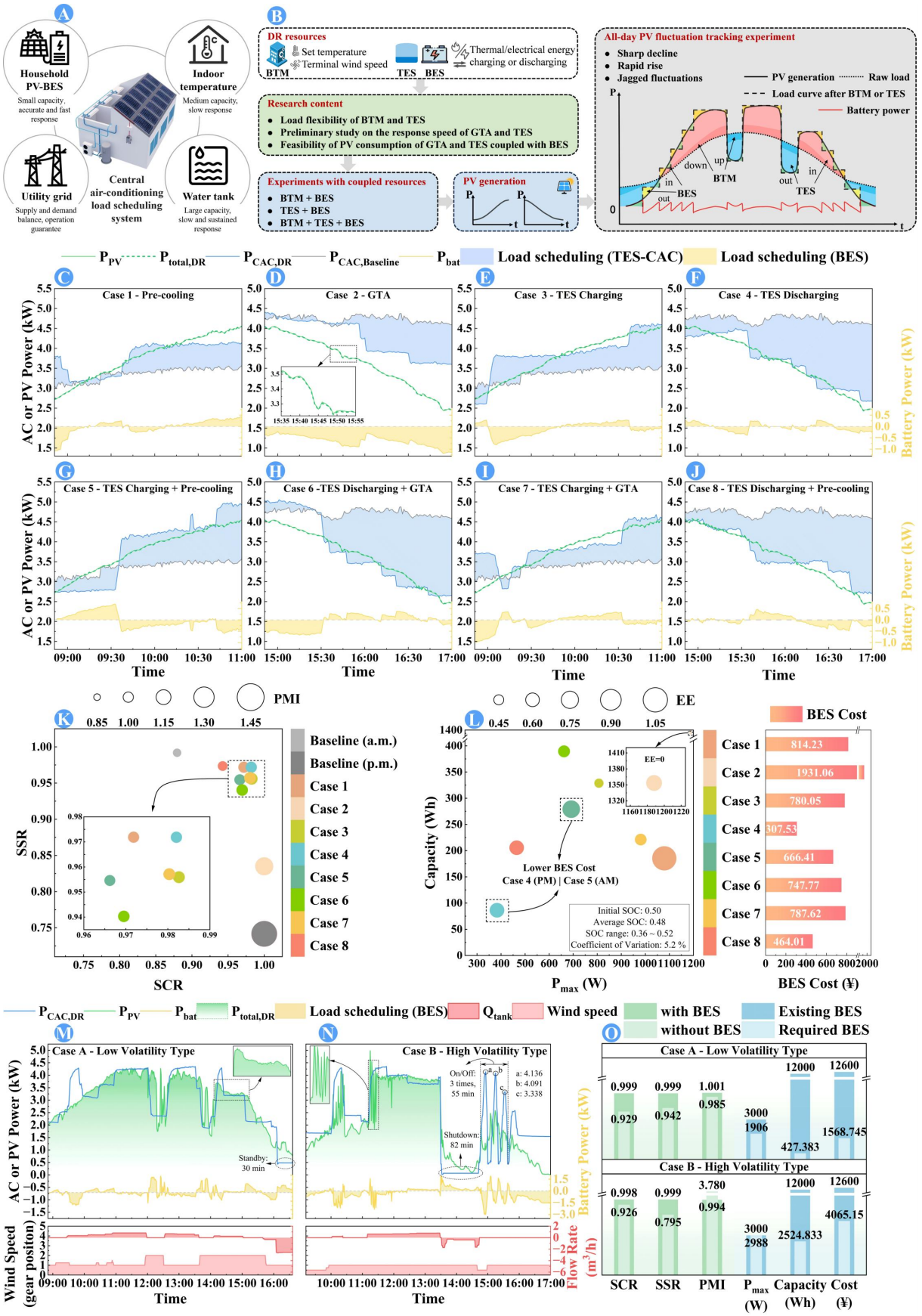

Figure 1. Summary of experimental results on the coordinated scheduling mechanism and performance on PV tracking of the hybrid energy storage CAC system. (A) Principle of the load scheduling mechanism. (B) Research process. (C-F) Power curve of thermal-side single DR strategies combined with BES. (G-J) Power curve of thermal-side coordinated DR strategies combined with BES. (K) PV utilization performance for each case. (L) BES operating efficiency and capacity calculations for each case. (M and N) Power curves and strategy implementation for full-day PV tracking. (O) Overall performance of all-day PV tracking.

The PV curve in Case A covered a relatively complete ramp-up and ramp-down process. In the initial ramp-up phase, tracking was achieved through wind speed regulation alone, with response time reduced from 17 minutes (pre-cooling) to 6 minutes. With the TES charging coupling, power rapidly rose above 4 kW and then gradually stabilized at about 4.2 kW under wind speed feedback by midday. After 12:17, PV power dropped sharply to 1.74 kW, approaching the 1.5 kW start-stop threshold. To avoid it, an interactive buffering strategy was employed (stopping TES charging while increasing wind speed). During power recovery, interactive control prevented excessive increases, allowing close following of PV output. A second sudden change was handled similarly. In the decline phase, gradual reduction of TES charging and wind speed achieved smooth tracking. Finally, wind speed decrease and TES discharging were coupled to bring CAC into standby mode at about 0.5 kW. Although thermal-side strategies showed flexibility, they struggled with sharp declines. With BES coordination, the maximum deviation between system and PV power was kept within 62.0 W.

Tracking the high volatility was more challenging. Initially, PV power was low. CAC operated at 1.7 kW due to low wind speed. When the curve spiked, wind speed increase and TES charging took effect. During a sharp decline, the drop was cushioned by shutting down TES charging while maintaining wind speed. Around 11:00, a second rapid rise occurred, causing a large PV surge. With coordinated wind speed increase and TES charging, a scheduling of 2.03 kW was achieved within 11 minutes. Due to cloud cover at 13:30, PV dropped to 0.1 kW. Full TES discharging replaced CAC operation to avoid start-stop cycles. After 14:30, a slow rise prompted an interactive buffering strategy (wind speed decrease and TES discharging), but load scheduling remained substantial. CAC still entered start-stop cycles. After startup, CAC operated at 1.55 kW, making low-power PV tracking difficult. After BES introduction, tracking improved significantly, with the maximum deviation maintained within 148.3 W.

The overall performance was further summarized in Figure 1O. In Case A, thermal-side flexible resources demonstrated strong PV tracking capability (SCR: 92.9%, SSR: 94.2%). With battery coordination, the matching accuracy was further improved, with both SCR and SSR reaching 99.9%, and the mismatch remaining within 0.1%. In Case B, the response speed of thermal-side DR strategies was insufficient under frequent sudden PV power changes, resulting in an SCR of 79.5% and a PMI of 3.780. The battery became an essential compensatory component. With battery participation, SCR, SSR, and PMI improved to 99.8%, 99.9%, and 0.994, respectively. Regarding BES, under low-volatility, the maximum capacity requirement was 427.383 Wh. The cost was ¥1,568.745, which was only 12.45% of the traditional configuration. Under high-volatility, the capacity requirement increased to 2,524.833 Wh, representing a 78.96% reduction compared to the original configuration. The cost reached ¥4,065.150. This indicated that thermal-side flexibility scheduling still required more refined optimization to further reduce the scheduling pressure on BES under high PV volatility for the specific conditions tested.

In summary, this letter systematically investigated coordination mechanisms among BTM, TES and BES in multi-scenario PV tracking. Thermal-side flexible resources leveraged their inherent scheduling characteristics for PV tracking, resulting in different operating modes, such as rapid large-scale or slow high-precision regulation. Significant synergistic benefits were achieved by integrating thermal-side flexible resources with micro-BES. During the rising phase of the PV curve, pre-cooling combined with TES charging demonstrated better adaptability alongside BES. In the afternoon, the synergy between TES discharging and BES was also effective.

However, PV volatility placed higher demands on system flexibility. Under the low-volatility condition, micro-BES was sufficient to ensure high-quality power matching. Under high-volatility, CAC experienced prolonged downtime and frequent start-stop cycles. This could reduce PV consumption, stress batteries, and damage the compressor. The optimal trade-off was to avoid start-stops and limit downtime to balance unit longevity, PV integration, and comfort. Given that the experiments were conducted only under typical weather conditions, further validation is needed to confirm the applicability of these results to other climate zones. Nevertheless, this letter provided experimental evidence for the optimized utilization of flexible resources through the synergy of micro-BES in buildings.

REFERENCES

1. Xiang Y., Li L., Li R., et al. (2024). Design flexible renewable energy penetrated power system to address long-run and short-run interactive inference. *Innov. Energy* **1**:100042. DOI:10.59717/j.xinn-energy.2024.100042
2. Liang S., Jin X., Jia H., et al. (2026). Bi-level Optimization of Residential Community Energy Systems: Space Heating and DHW Loads under Multi-Energy Pricing. *Energy Use* **2**:100036. DOI:10.59717/ipj.energy-use.2026.100036
3. European Commission (2020). COMMUNICATION FROM THE COMMISSION TO THE EUROPEAN PARLIAMENT, THE COUNCIL, THE EUROPEAN ECONOMIC AND SOCIAL COMMITTEE AND THE COMMITTEE OF THE REGIONS. EUR-Lex, https://eur-lex.europa.eu/legal-content/EN/TXT/?uri=CELEX%3A52020DC0662
4. Alam M.A., Irshad K., Rehman S., et al. (2025). Recent developments in renewable energy assisted cold thermal energy storage air conditioning systems. *J. Energy Storage* **127**:117124. DOI:10.1016/j.est.2025.117124
5. Belloni E., Buratti C., Casini M., et al. (2026). Thermo-electric storage systems in renewable energy communities: Modeling challenges and perspectives. *J. Energy Storage* 176:123344. DOI:10.1016/j.est.2026.123344
6. Sun L., Hu Z., Nitta M., et al. (2025). Bayesian robust reinforcement learning for coordinated air conditioning and energy storage system control in high-performance residential buildings under forecast uncertainty. *Appl. Energy* **400**:126571. DOI:10.1016/j.apenergy.2025.126571
7. Li S., Li Y., Wang M., et al. (2025). A hierarchical multi-objective co-optimization for capacity design and control strategy of PV air conditioning coupled with load flexibility and batteries. *J. Energy Storage* **134**:118080. DOI:10.1016/j.est.2025.118080
8. Liu Y., Liu H., Yang K., et al. (2026). Design and performance evaluation of a building-integrated multi-component energy system with PV/T and thermal storage for electricity and heat supply. *Energy* **353**:140996. DOI:10.1016/j.energy.2026.140996
9. Ahmed S., Knehr K.W., Effat M.B., et al. (2026). Designing automotive battery packs: sensitivity, case studies and insights using BatPaC. *J. Power Sources* **671**:239491. DOI:10.1016/j.jpowsour.2026.239491
10. Ye A., Liu S., Zhang T., et al. (2025). Experimental study on flexible energy use feature of multi-split air-conditioning system with different control schemes in summer. *Energy Build.* **342**:115875. DOI:10.1016/j.enbuild.2025.115875

FUNDING AND ACKNOWLEDGMENTS

The work was sponsored by the National Natural Science Foundation of China (52578124, 52278104), Guangdong Basic and Applied Basic Research Foundation (2025A1515012092), the Scientific Research Fund of Hunan Provincial Education Department (24B0042), and Furong Plan Youth Talent Program (2025QT-57).

AUTHOR CONTRIBUTIONS

Yuchen Liu: Writing - original draft, Investigation. Jingyu Cao: Writing - original draft, Writing - review & editing, Supervision, Funding acquisition. Qiliang Wang: Methodology, Conceptualization. Jian Li: Visualization, Resources. Gang Pei: Methodology. Jie Ji: Visualization. Jinqing Peng: Writing - review & editing, Funding acquisition. All authors contributed to and approved the final version of the manuscript.

DECLARATION OF INTERESTS

The authors declare no competing interests.